larator points to the most probable process: transformation of a Langmuir wave into an electromagnetic wave upon scattering by ion-plasma noise. Special notice should be taken of the Raman type of the radiated superthermal spectrum, in which the width of the individual satellites is $\ll \omega_{pi}$.[6] Such a discrete character of the spectrum can be possessed only by solitons.

We note in conclusion that the tail on the particle distribution function in a magnetized plasma is a phenomenon that is much more natural and therefore more frequently encountered than a beam, which usually must be produced by a special device. Usually the tail carries an appreciable fraction of the electric current with anomalously low resistance, and thereby strongly influences the hydrodynamic properties of the plasma. Therefore the interaction of the runaway electrons of the tail with the considered solitons, which in addition to the aforementioned resonance takes place also at resonances with multiple cyclotron frequencies, calls for further study.

[1]B. B. Kadomtsev, in: Nelineĭnye volny (Nonlinear Waves), Nauka, 1979, p. 131.
[2]A. V. Longinov, N. F. Perepelkin, and V. A. Suprunenko, Fizika plazmy **2**, 636 (1976) [Sov. J. Plasma Phys. **2**, 344 (1976)].
[3]A. V. Stefanovskiĭ, Nuclear Fusion **5**, 215 (1965).
[4]S. D. Fanchenko, B. A. Demidov, N. I. Elagin, and N. F. Perepelkin, Dokl. Akad. Nauk SSSR **183**, 77 (1968) [Sov. Phys. Doklady **13**, 1128 (1969)].
[5]A. G. Dikiĭ, O. S. Pavlichenko, N. F. Perepelkin, and V. A. Suprunenko, in: Voprosy atomnoĭ nauki i tekhniki (Problems of Atomic Science and Engineering), No. 1, Khar'kov, Khar-kov Physicotech. Inst. Ukr. Acad. Sci., 1974, p. 22.
[6]A. G. Dikiĭ, Yu. K. Kuznetsov, O. S. Pavlichenko, V. K. Pashnev, N. F. Perepelkin, V. A. Suprunenko, and V. T. Tolok, Research into Plasma Physics and Controlled Thermonuclear Fusion, IAEA, Vienna, 1975, p. 45.
[7]V. I. Petviashvili, Fizika plazmy **1**, 28 (1975) [Sov. J. Plasma Phys. **1**, 15 (1975)].
[8]V. E. Zakharov, Zh. Eksp. Teor. Fiz. **62**, 1745 (1972) [Sov. Phys. JETP 35, 908 (1972)].
[9]S. V. Antipov, M. V. Nezlin, E. I. Snezhkin, A. S. Trubnikov, *ibid*. **76**, 1571 (1979) [**49**, 797 (1979)].
[10]B. B. Kadomtsev and O. P. Pogutse, *ibid*. **53**, 2025 (1967) [**26**, 1145 (1968)].
[11]A. B. Mikhaĭlovskiĭ, Teoriya plazmennykh neustoichivosteĭ (Theory of Plasma Instabilities), Vol. 1, Atomizdat, 1975, p. 158.
[12]V. I. Petviashvili, Fizika Plazmy **2**, 469 (1976) [Sov. J. Plasma Phys. **2**, 257 (1976)].
[13]V. V. Parail and O. P. Pogutse, Nuclear Fusion 18, 202 (1978).
[14]N. F. Perepelkin, V. A. Suprunenko, V. I. Petviashvili, and M. P. Vasil'ev Eighth European Conf. on Controlled Thermonucl. Fusion and Plasma Phys., No. 2, Prague, 1977, p. 144.
[15]J. H. Hutchinson and D. S. Komm, Nuclear Fusion **17**, 1077 (1977).
[16]P. Brossier, *ibid*. **18**, 8 (1978).
[17]P. Brossier, M. Churet, J. Gratadeur, and Y. Tosolini, EUR-CEA-FC-995, Dec. 1978, p. 107.

Translated by J. G. Adashko

Theoretical study of the hydrodynamics of spherical targets taking the refraction of the laser radiation into account

Yu. V. Afanas'ev, E. G. Gamaliĭ, N. N. Demchenko, O. N. Krokhin, and V. B. Rozanov

P.N. Lebedev Physical Institute, Academy of Sciences of the USSR

(Submitted 10 December 1979; resubmitted 29 April 1980)
Zh. Eksp. Teor. Fiz. 79, 837–849 (September 1980)

We consider the problem of the refraction and absorption of laser light in a dispersing spherically symmetric plasma. The process of the interaction of the radiation with the medium is described by the Maxwell equations for heating radiation and the hydrodynamical equations with electron thermal conductivity. The proposed model takes into account absorption mechanisms: inverse bremsstrahlung, and anomalous and resonance absorption. We give a numerical solution of these equations for glass shells of diameter of about 100 μm and laser pulse power of about 5×10^{10}W with a length of about 2 ns. We pay our main attention to a study of the absorption of the laser light in the target. We compare the results of our calculations with experimental data.

PACS numbers: 52.25.Ps

1. STATEMENT OF THE PROBLEM

One of the problems arising when one irradiates spherical targets with laser light is the determination of the fraction of energy of the laser pulse which is spent on heating and compressing the target. In a previous paper[1] we considered such a problem for the case of a plane target and normal incidence of the light. In the present paper we use a similar approach for the case of spherical targets. We note that experimentally in spherical heating it is impossible to establish an absolutely symmetrical spherical irradiation of the target. This follows, for example, from the fact that the solid angle filled by the focusing optics must be less than 4π.

Under such conditions an important effect which may strongly increase the loss of laser energy is the refrac-

0038-5646/80/090425-07$02.40

tion of laser light in the target corona. In connection with the difficulty of solving the complete three-dimensional problem of the dispersion of a target irradiated by a finite number of beams it is natural to consider in the first stage the problem of the determination of the energy released by the laser, averaged over the angles, assuming a spherically symmetric hydrodynamic dispersal of the target.

The initial set of equations has the form

$$\frac{\partial}{\partial t}\left(\frac{1}{\rho}\right)=\frac{\partial}{\partial m}(r^2u),\quad \frac{\partial r}{\partial t}=u, \tag{1}$$

$$\frac{\partial u}{\partial t}=-r^2\frac{\partial}{\partial m}\left[p-\mu\rho\frac{\partial}{\partial m}(r^2u)\right]-3ur\frac{\partial\mu}{\partial m}, \tag{2}$$

$$\frac{\partial\mathscr{E}_e}{\partial t}=-p_e\frac{\partial}{\partial m}(r^2u)+\frac{\partial}{\partial m}\left(\varkappa\rho r^4\frac{\partial T_e}{\partial m}\right)-Q-\frac{\partial q}{\partial m}, \tag{3}$$

$$\frac{\partial\mathscr{E}_i}{\partial t}=-\left[p_i-\mu\rho\frac{\partial}{\partial m}(r^2u)\right]\frac{\partial}{\partial m}(r^2u)+Q-3\mu\frac{\partial}{\partial m}(r^2u), \tag{4}$$

$$\operatorname{rot}\mathbf{E}=i\omega\mathbf{H}/c,\quad \operatorname{rot}\mathbf{H}=-i\omega\varepsilon\mathbf{E}/c, \tag{5}$$

$$q=\frac{r^2}{4\pi}\int_{(4\pi)}S_r\,d\Omega,\quad \mathbf{S}=\frac{c}{16\pi}([\mathbf{E}\times\mathbf{H}^*]+[\mathbf{E}^*\times\mathbf{H}]), \tag{6}$$

where u is the velocity, ρ the density, r the Euler coordinate, m and t Lagrangian variables, $p=p_e+p_i$ the total pressure, $p_e=(\gamma-1)A_e\rho T_e$ and $p_i=(\gamma-1)A_i\rho T_i$ the electron and ion pressure, respectively, $\gamma=5/3$ the adiabatic constant, $\mu=(4/3)\eta_0T_i^{5/2}$ the ion viscosity coefficient, $\mathscr{E}_e=A_eT_e$ and $\mathscr{E}_i=A_iT_i$ the internal energy of the electron and ion component, T_e and T_i the electron and ion temperature, $\varkappa=\varkappa_0T_e^{5/2}$ the electron thermal conductivity coefficient, $Q=Q_0\rho(T_e-T_i)T_e^{3/2}$ the speed of the energy exchange between ions and electrons, **E** and **H** the complex electrical and magnetic field vectors, $\varepsilon=\varepsilon'+i\varepsilon''$ the complex permittivity of the plasma, $\varepsilon'=1-a_0\rho$, $\varepsilon''=b_0\rho^2/T_e^{3/2}$ (a_0, b_0 known constants), $d\Omega$ an element of solid angle on the sphere, **S** the Poynting vector, q the flux of light through a sphere of radius r per steradian. If the anomalous absorption is taken into account, ε'' is determined by the effective collision frequencies given earlier.[1]

2. SOLUTION OF THE MAXWELL EQUATIONS

The simultaneous solution of Eqs. (1) to (5) reduces to a successive integration of the Maxwell equations for given density $\rho(r)$ and temperature $T_e(r)$ distributions, and hence also $\varepsilon(r)$ distributions. Let the laser beam be focused by an ideal lens such that the optical axis goes through the center of the target while the focus lies in an arbitrary point F behind the target (Fig. 1), L is the distance between the target center and the lens, R the maximum radius of the corona, r_{cr} the radius of the critical surface. Normally the characteristic values of R and r_{cr} are appreciably larger than the wavelength of the laser light so that it is natural to use as the initial approximation for the solution of Eqs. (5) the geometric optics approximation (see, e.g., Ref. 2)

$$\theta(r)=R\sin\theta_0, \tag{7}$$

where $n(r)$ is the refractive index, $\theta(r)$ the angle between the ray direction and the gradient of ε, and the

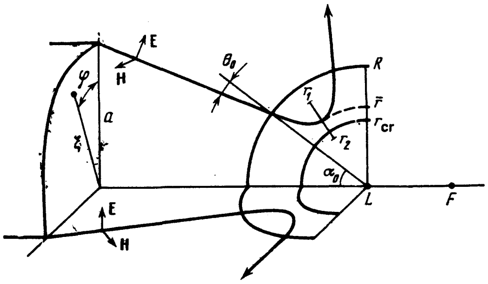

FIG. 1. Beam focusing and ray paths in a laser target corona.

meaning of the angle θ_0 is clear from Fig. 1. Using (7) one can construct the ray path and determine the reflection point $\bar{r}$ in which $\sin\theta(\bar{r})=1$.

The next approximation is connected with splitting off the vicinity (r_1, r_2) of the reflection point such that $(r_1-\bar{r})\approx(\bar{r}-r_2)$ and equals several wavelengths.[1] Furthermore, using the fact that the wavelength is small compared to r_{cr} we neglect the curvature of the layer (r_1, r_2) and for a given ray consider the wave problem of oblique incidence of light onto a plane layer (r_1, r_2) (see, e.g., Ref. 3). Thus, the reflection point plays a subsidiary role, namely, it serves to split off a neighborhood in which the wave problem is considered. We can thus put $n(r)=[\varepsilon'(r)]^{1/2}$ in (7). The boundary conditions for the wave problem are: in the point r_1 matching with the geometric optics approximation and for $r<r_2$ the condition for wave damping.

We can connect with the ray considered a certain area $\xi d\xi d\varphi$ in the plane of the lens, and, hence, a certain incident energy flux $dq_n=I(\xi)\xi d\xi d\varphi$ [$I(\xi)$ is the intensity in the laser beam] and we can evaluate the energy-release distribution from this flux as function of the radius in the corona. Moreover, splitting the electric field vector into components in the plane of incidence and at right angles to it we can integrate the energy release over the angle φ and consider solely a two-dimensional problem: one dimension—along the ray in the appropriate wave problem and the second one—along ξ, i.e., a division of the laser beam into a set of concentric areas $2\pi\xi d\xi=\pi d\xi^2$. This is the general scheme of the calculations.

We now give the basic equations and relations. The ray path is constructed by using the relation

$$\alpha=\alpha_0+\int_r^R\frac{R\sin\theta_0\,dr}{r(n^2r^2-R^2\sin^2\theta_0)^{1/2}}. \tag{8}$$

The meaning of the angle α is clear from Fig. 1. A length element of the ray along the incident branch is

$$dl=-\frac{dr}{[1-(R\sin\theta_0)^2/(rn)^2]^{1/2}}\quad(dr<0). \tag{9}$$

If we take anomalous absorption into account it is necessary to know the change in the electric field amplitude along the incident branch of the ray:

$$|E|^2=\frac{|E|_0^2}{n}\exp\left(-\int_0^l k\,dl\right)\frac{\Delta S_0}{\Delta S}, \tag{10}$$

where $k=2\omega\,\mathrm{Im}\,\varepsilon^{1/2}/c$ is the absorption coefficient, ω the frequency of the laser light, c the light speed, and

ΔS the cross-section area of the light beam tube. The index zero indicates a quantity at the point of entry of the ray into the corona. Varying (8) with respect to α_0 and θ_0 we get

$$\frac{\Delta S}{\Delta S_0}=\frac{r^2\sin\alpha\cos\theta}{R^2\sin\alpha_0\cos\theta_0}\left(1+\frac{\delta\theta_0}{\delta\alpha_0}\int_r^R\frac{R\cos\theta_0 n^2 r\,dr}{(n^2r^2-R^2\sin^2\theta_0)^{3/2}}\right),\qquad(11)$$

where the derivative $\delta\theta_0/\delta\alpha_0$ is easily determined for given F and L.

We now turn to the wave equations. As we consider a problem for a plane layer it is convenient to introduce Cartesian coordinates: z along the radius in the direction to the center of the target, x at right angles to the plane of incidence, and y in the plane of incidence (the plane of incidence is the plane through the ray and the optical axis). We then get from (5) for an s-polarized wave ($E_y=E_z=0$, $H_x=0$)

$$\frac{dG_y}{dz}-\frac{i\omega}{c}(\varepsilon-\bar{\varepsilon}')F_x=0,\quad \frac{dF_x}{dz}-\frac{i\omega}{c}G_y=0,\qquad(12)$$

$$G_z=-(\bar{\varepsilon}')^{1/2}F_x,\qquad(13)$$

where $\mathbf{G}$ and $\mathbf{F}$ are functions depending solely on z,

$$\mathbf{E}=\mathbf{F}(z)\exp\left(\frac{i\omega}{c}(\bar{\varepsilon}')^{1/2}y\right),\quad \mathbf{H}=\mathbf{G}(z)\exp\left(\frac{i\omega}{c}(\bar{\varepsilon}')^{1/2}y\right),\quad \bar{\varepsilon}'=\varepsilon'(\bar{r}).$$

Similarly, for p-polarization ($E_x=0$, $H_y=H_z=0$)

$$\frac{dG_x}{dz}+\frac{i\omega}{c}\varepsilon F_y=0,\quad \frac{dF_y}{dz}+\frac{i\omega}{c}\frac{\varepsilon-\bar{\varepsilon}'}{\varepsilon}G_x=0,\qquad(14)$$

$$F_z=(\bar{\varepsilon}')^{1/2}G_x/\varepsilon.\qquad(15)$$

We consider Eqs. (12). By analogy with Ref. 1 we write the field in the form

$$F_x=P_\perp+R_\perp=P_\perp(1+V_\perp),\qquad(16)$$

$$G_y=\beta(P_\perp-R_\perp)=\beta P_\perp(1-V_\perp),\qquad(17)$$

where $\beta=(\varepsilon-\bar{\varepsilon}')^{1/2}$, $P_\perp$ is the "incident wave," $R_\perp$ the "reflected wave", and $V_\perp=R_\perp/P_\perp$ the "reflection coefficient." Substituting (16) and (17) in (12) we get an equation for $V_\perp$:

$$\frac{dV_\perp}{dz}=-2\frac{i\omega}{c}\beta V_\perp+\frac{1}{2\beta}\frac{d\beta}{dz}(1-V_\perp^2).\qquad(18)$$

Similarly we also introduce into (14) the corresponding functions:

$$F_y=\gamma(P_\parallel+R_\parallel)=\gamma P_\parallel(1+V_\parallel),\qquad(19)$$

$$G_x=-P_\parallel+R_\parallel=P_\parallel(-1+V_\parallel),\quad \gamma=(\varepsilon-\bar{\varepsilon}')^{1/2}/\varepsilon\qquad(20)$$

and we get an equation for $V_\parallel$:

$$\frac{dV_\parallel}{dz}=-2\frac{i\omega}{c}\beta V_\parallel-\frac{1}{2\gamma}\frac{d\gamma}{dz}(1-V_\parallel^2).\qquad(21)$$

We get the boundary conditions for (18) and (21) from the condition for wave damping when $z>z_2$ (in Fig. 1 the point r_2 corresponds to the point z_2, while r_1 corresponds to z_1):

$$V_\perp(z_2)=V_\parallel(z_2)=0.\qquad(22)$$

We integrate Eqs. (18) and (21) numerically. We do not give the equations for $P_\perp$ and $P_\parallel$ which one gets easily from (12) and (14).

Having determined $V_\perp(z_1)$ and $V_\parallel(z_1)$ we turn to the region $r\geq r_1$, where we have for the reflected coefficients

$$|V_{\perp,\parallel}(r)|^2=|V_{\perp,\parallel}(r_1)|^2\exp\left(2\int_{r_1}^{r}k\frac{dl}{dr}dr\right).\qquad(23)$$

We consider the case of a linearly polarized laser beam. The differential energy flux (corresponding to the area $\xi d\xi d\varphi$) into a sphere of radius r can then be written in the form

$$dq(r)=dq_n(r)\,(1-|V_\perp(r)|^2\sin^2\varphi-|V_\parallel(r)|^2\cos^2\varphi),$$
$$dq_n(r)=dq_n(R)\exp\left(\int_r^R k\frac{dl}{dr}dr\right).\qquad(24)$$

Integrating (24) over φ we get

$$\Delta q(r)=\Delta q_n(r)\,[1-{}^1/_2(|V_\perp(r)|^2+|V_\parallel(r)|^2)\,].\qquad(25)$$

We note that Eq. (25) for the flux, averaged over the angle φ, is valid not only for linear, but also for elliptical polarization, and also for unpolarized radiation.

The matching of the quasi-classical and the wave solutions in the point r_1 proceeds using the condition that the flux be continuous. Starting from the wave solution we write down the radial current density (the Poynting vector) $S_z(z)$ and after that normalize it to the flux through the area $d\sigma$ defined by the condition

$$dq(r_1)=S_z(z_1)\,d\sigma.\qquad(26)$$

Without going into details we make some remarks in connection with resonance absorption. If we are interested not so much in the maximum longitudinal field at the critical surface, but in the magnitude of the laser energy absorbed due to that mechanism, the latter does not depend only on which collision frequency limits the growth of the field. This problem was studied in Ref. 4 where it was shown that one can for the determination of the transfer of energy from the incident wave to the plasma use the limit as $\nu_e\to 0$, where ν_e is the electron collision frequency.

We note also the interesting approach to a solution of Eqs. (5) in a spherically symmetric plasma which is based upon the method of expanding the potentials in spherical harmonics.[5,6] Such a method offers great possibilities for taking the wave properties of light into account. However, in view of the difference between hydrodynamic and wave scales, the inclusion of this method in the calculation of the evolution of a target is difficult. The model considered by us is a compromise between the possibilities of a computational technique and the number of physical phenomena taken into account. Equations (1) to (4) were solved by different methods using a completely conservative difference scheme.[7] A matching of the hydrodynamic and wave scales is accomplished by means of interpolation in the vicinity of the critical point: of the density ρ which is linear in the variable m which corresponds to an exponential interpolation in the variable r, and of the temperature T_e which is linear in the variable r.

3. RESULTS

We consider the results of a calculation of a variant which was chosen to illustrate the model considered. A solid target of DT ice with an initial radius $R_0=100\ \mu$m was irradiated by twelve beams, the diameter of each beam $2a=4$ cm (the intensity was constant over the beam cross-section), $F=8$ cm, $F-L=500$ μm, and the total power of the beams equalled 1.2×10^{11} W and was independent of the time (infinitely long pulse). We give in Fig. 2 the behavior of the differential fraction δ of the loss flux,

$$\delta(\xi,\ \varphi)=\delta(\xi,\ 0)\cos^2\varphi+\delta(\xi,\ \pi/2)\sin^2\varphi,$$

along the beam cross-section at time $t=0.87$ ns after the start of the action of the pulse in the case of anomalous absorption and the case of only binary electron collisions (classical absorption). In the same figure we show also the integral fraction Δ of the loss flux (Δ is the average of the quantity δ over the beam cross-section).

It is clear from Fig. 2(a) that the central part of the beam lies in the band of anomalous absorption, which is appreciably larger than the classical absorption, so that δ undergoes a strong change at $\xi\approx0.8$ cm. From Fig. 2(b) one sees a qualitative deviation of the function $\delta(\xi,\varphi)$ from the anomalous absorption case. The $\delta(\xi,\varphi=0)$ curve has a sharply pronounced minimum that corresponds to the angle of incidence of the ray which is an optimum for resonance absorption. However, in the case of anomalous absorption the radiation undergoes strong absorption even before it approaches the critical surface, so that the role of resonance absorption is there insignificant. It also follows from Fig. 2(b) that under the conditions considered (lens aperture, light wavelength, characteristic density gradient) the role of the resonance absorption is small in the total balance over the beam cross-section, since the area in the beam is $\propto\xi^2$.

We note that the role of the resonance absorption increases with increasing aperture of the focusing optics and wavelength. We give in Fig. 3 the fraction of the loss current Δ as function of the shift of the target from the focus in the case of classical absorption and with the anomalous absorption taken into account. The density and temperature profiles are taken at the same time ($t=0.87$ ns). It is clear from the figure that curve 1, which corresponds to the classical absorption, has a minimum caused by resonance absorption. We note that similar behavior is also shown in the work of Erkkila.[5]

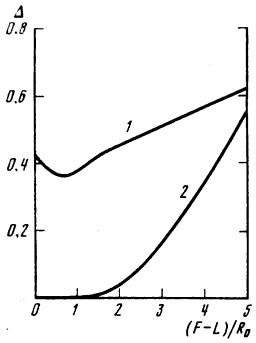

FIG. 3. The loss flux fraction as function of the shift of the target from the focus in the case of classical (curve 1) and anomalous (curve 2) absorption.

In Fig. 4 we depict the structure of the electromagnetic field in the region of maximum resonance absorption for a classical collision frequency ($t=0.87$ ns). This region corresponds to the minimum of the $\varphi=0$ curve in Fig. 2(b). We give a comparison of the thermal pressure in the plasma in the critical point p_{cr} and the electromagnetic pressure at resonance $p_r^{em}=|E|_r^2/16\pi$ (Fig. 4; we remind ourselves that the light flux at the target surface in our example is $\approx10^{14}$ W/cm^2):

$$p_{cr}=p_{e\,cr}+p_{i\,cr}=1.4\cdot10^{12}\ \text{erg/cm}^3\quad(p_{e\,cr}/p_{i\,cr}=3.6),$$
$$p_r^{em}=5.46\cdot10^{11}\ \text{erg/cm}^3,\quad p_{cr}/p_r^{em}=2.6.$$

We note that this estimate refers to a relatively small part of the target surface where the resonance field is large. In the other parts of the target the ratio p_{cr}/p_r^{em} is $>10^2$.

A comparison show that the thermal pressure is larger than p_r^{em}, but that they can be of comparable order of magnitude, and it is, in principle, necessary to study the effect of p_r^{em} on the plasma dynamics. The problem is complicated by the fact that the resonance shifts with mass and affects the Lagrangian of the particle during a time interval which is considerably shorter than the characteristic hydrodynamic time scale. Therefore, the changes caused by the pressure p_r^{em} are themselves dependent on the dynamics of the corona, which is determined by the pressure p_f at the front of the thermal wave, with $p_f>p_{cr}$. In the example considered $p_f=10^{13}$

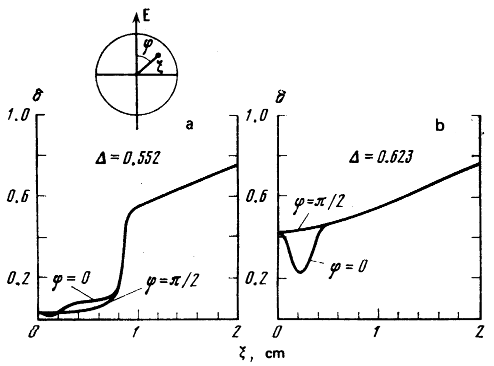

FIG. 2. Behavior of the differential fraction of the loss flux across the beam cross-section for the cases of: a) anomalous absorption, b) classical absorption.

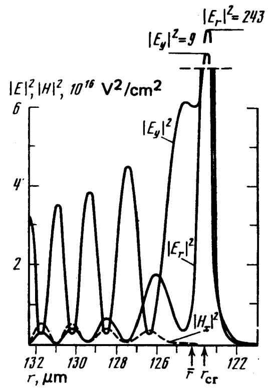

FIG. 4. Structure of the electromagnetic field in the region of maximum resonance absorption in the case of a classical collision frequency.

erg/cm^3. In any case, the problem of the effect of the electromagnetic pressure needs a special study.

We give the results of a calculation of the variants connected with experiments on the "Kal'mar" facility.[8] The target is a glass shell filled with D_2 gas of density 5.4×10^{-3} g/cm^3. The radius of the shell is 70 μm, its thickness 2.2 μm. The diameter of the laser beam is 2 cm, $F=10$ cm. The target was positioned such that the diameter of the beam cross-section in the plane of the target was 150 μm. The intensity over the beam cross-section was assumed to be constant, the temporal pulse shape was chosen in the form of a trapeze with base 2.5 ns and top 1.5 ns, and a rise time 0.5 ns. The energy in the pulse $E_{\text{pulse}}\sim 60$ to 100 J (neodymium laser).

We show in Fig. 5 the behavior of the ratio of the cross-section of a light-beam tube in the incident radiation to the corresponding cross-section in the refracted radiation at the radius of the vacuum chamber. The abscissas are the angles between the optical axis and the refracted rays. It follows from this behavior that if we put a receiver with small aperture 2β on the optical axis on the opposite side of the beam, the contribution from the refracted radiation from the other beams will be small in the given receiver (in the "Kal'mar" set-up there are 9 beams, $\beta=14°$). Hence, if an appreciable fraction of the light falls upon the receiver one can conditionally speak of the light passed beyond the target, in other words, of refraction at small angles.

Figure 5 is drawn for the case $E_{\text{pulse}}=101$ J and $t=1.31$ ns, when the radius of the critical surface has its minimum value. It is clear from the figure that the radiation cannot be incident upon the receiver, but in the experiment the fraction of passed energy $\delta_t\approx 0.3$ ($\delta_t=E_t/E_{\text{pulse}}$, E_t is the energy passed through the target). The fraction of absorbed energy $\delta_{\text{abs}}=E_{\text{abs}}/E_{\text{pulse}}$ is 0.55 in the calculations. This value was obtained assuming classical absorption and an average degree of ionization of the glass atoms $Z_{\text{gl}}=8$. If $Z_{\text{gl}}=10$, we have $\delta_{\text{abs}}=0.57$ (in what follows we put $Z_{\text{gl}}=8$). If the anomalous absorption is taken into account and $Z_{\text{gl}}=10$ we obtained $\delta_{\text{abs}}=0.86$. In the experiment $\delta_{\text{abs}}\approx 0.3$.

The difference between the experimental values and those in the calculations, and above all, in the fraction of energy passed required a more detailed consideration of the experimental conditions. Due to the divergence of the radiation the actual intensity distribution of the radiation in the target plane differs from the "shelf" assumed in the calculations. The radiation can be divided into two components; one with small divergence, producing in the target plane a Gaussian intensity distribution with a characteristic radius of 70 μm, and with large divergence, producing wings.

The intensity in the target plane was given in the form

$$I(s)=I_0\exp[-(s/a)^2]+I_1, \tag{27}$$

where s is the distance from the optical axis, $0\leq s\leq 350$ μm, $a=70$ μm, $I_1/I_0=1.72\times10^{-2}$, with 70% of the total flux contained in the radiation with small divergence. The calculations under such conditions give, assuming classical absorption $\delta_t=0.28$, $\delta_{\text{abs}}=0.38$, which agree with the experimental values.

We give in Fig. 6(a) the time-dependence of the fraction of loss flux and the Rt diagrams of the critical surface and the boundary of the D_2 gas with the glass. The critical surface initially moves from the center, owing to the evaporation of the external part of the shell, and later it moves with the shell towards the center. The fraction of loss flux Δ initially decreases steeply due to the reduction in the density gradient in the corona, and also due to the increase in the radius of the critical surface. Afterwards Δ increases due to the decrease in the radius of the critical surface. Moreover, notwithstanding the fact that after the collapse the critical surface moves from the center, Δ continues to increase, reaches a maximum, and then again decreases. The reason is that the shell moving away from the center produces in the corona a perturbation that leads to an increase in the density gradient near the critical surface and to an increase in reflection.

We show in Fig. 6(b) the analogous behavior for a shell of diameter 120 μm and thickness 1.4 μm. It shows also the experimental points of the Rt diagram of the critical surface, taken from Ref. 8. A large difference between the experimental value of the critical radius and the calculated one is observed only in the initial stage of the dispersal and indicates that we describe

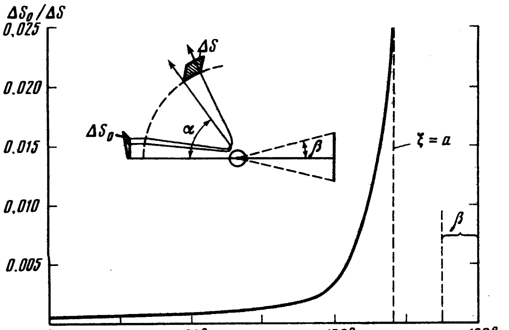

FIG. 5. Relative change in the cross-section of the light beam tube in the refracted radiation as function of the angle of refraction ($t=1.31$ ns, $r_{\text{cr}}=58$ μm).

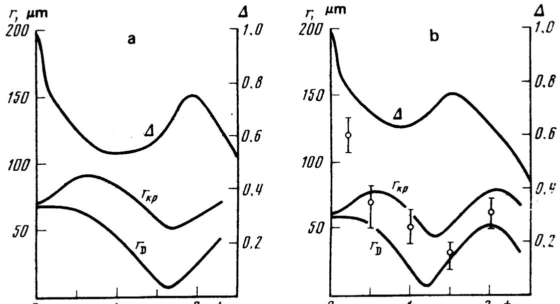

FIG. 6. Rt diagrams of the motion of the critical surface (r_{cr}) and the boundary of the D_2 gas with the glass (r_D); evolution of the loss flux fraction (Δ). a) $2R_0=140$ μm; $\Delta R_0=2.2$ μm, $E_{\text{pulse}}=62$ J; b) $2R_0=120$ μm, $\Delta R_0=1.4$ μm, $E_{\text{pulse}}=62$ J.

poorly the initial stage of corona formation. It follows from the calculations that at time $t = 0.23$ ns the plasma boundary has the same radius 120 μm as the experimental value of the critical radius.

Under the conditions of the experiment considered, a better agreement for the fraction of absorbed energy is reached when we use the classical absorption mechanism; taking anomalous mechanisms into account leads to an overestimate of the absorption. A study of curves analogous to those given in Fig. 6(b) showed that under the conditions considered the role of resonance absorption in the total energy balance is small. A comparison of the thermal and electromagnetic pressures for the variant given in Fig. 6(a) ($t = 0.97$ ns) gives

$$p_{cr} = 1.05 \cdot 10^{12}\ \text{erg/cm}^3, \quad p_{cr}/p_r^{em} = 25 \quad (p_{e\,cr}/p_{i\,cr} = 16, \quad p_f/p_{cr} = 3.24).$$

We give in Fig. 7 the fraction of absorbed energy as function of the target diameter, obtained by calculations and in a series of experiments on the heating and compression of shell targets on the "Kal'mar" facility.[9] The focusing conditions remained unchanged when the target diameter was changed and the diameter of the laser beam cross-section at the target was, according to (27), ~140 μm. It is clear from the figure that for target diameters 80 to 180 μm the theoretical and experimental values are in good agreement. For target diameters well above the laser beam diameter the theoretical curve lies somewhat above the experimental values, due to the fact that the plasma dispersal is not spherically symmetric. For very large target diameters each laser beam forms its own jet, which leads to increased losses due to refraction. A quantitative study of the problem in that case is greatly more complicated. However, to reach maximum compressions of the thermonuclear fuel, such conditions of irradiation are of no interest.

We shall dwell in more detail on the resonance absorption mechanism in a spherical target. As a result of resonance absorption epithermal electrons are generated[4] which may heat up the whole target and change the heating and compression regime of the target. We determine the coordinate ξ_r of the ray for which the condition for maximum resonance absorption is satisfied. The characteristic region of the beam which takes part in the resonance absorption lies then in the range $0 \leq \xi \leq 2\xi_r$ [see Fig. 2(b)]. If $\xi_r/\xi_0 \ll 1$ (ξ_0 is the radius of the beam), only a small fraction of the beam close to

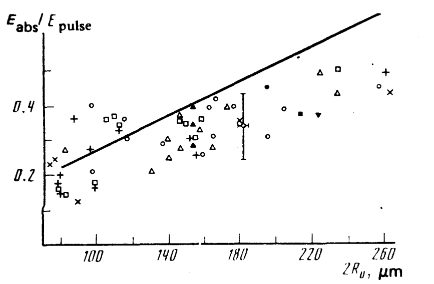

FIG. 7. Absorbed laser energy fraction as function of the target diameter under the experimental conditions in the "Kal'mar" facility. Curve: theory; points: experiment.

the optical axis takes part in the resonance absorption. When $\xi_r/\xi_0 \gg 1$ the resonance absorption is also small since the angles of incident of the rays are far from optimal. Appreciable resonance absorption is thus possible when $\xi_r/\xi_0 \sim 1$. The condition for maximum resonance absorption[10]

$$\tau = (\omega l/c)^{1/3} \sin \theta_{abs} = \tau_0 \approx 0.7$$

takes in the case considered by us the form

$$\varepsilon'(\bar{r}) = \tau_0^2 (c/\omega l)^{2/3}, \qquad l = (d\varepsilon'/dr)_{cr}^{-1}.$$

Furthermore, $p^2 = \varepsilon'(\bar{r})\bar{r}^2 \approx \varepsilon'(\bar{r}) r_{cr}^2$, where $p = R \sin\theta_0$ is the impact parameter of the ray. From similarity considerations it also follows that

$$\xi/(\xi^2 + F^2)^{1/2} = p\xi_0/r_{bt}F,$$

where r_{bt} is the radius of the laser beam in the plane through the center of the target.

Finally we get

$$\frac{\xi_r^2}{\xi_\cdot^2} = b\Big/\left[1 - b\left(\frac{\xi_0}{F}\right)^2\right], \quad b = \alpha\left(\frac{\lambda}{l}\right)^{2/3}\left(\frac{r_{cr}}{r}\right)^2, \qquad (28)$$

where λ is the wavelength in vacuo, α a numerical factor, $\alpha = 0.144$ when $\tau_0 = 0.7$. An analysis of numerical calculations shows that calculated values of ξ_r/ξ_0 are obtained from Eq. (28) at $\alpha = 0.17$ to 0.21, which corresponds to values $\tau_0 = 0.76$ to 0.84 (cf. Ref. 4). For instance, for the conditions of the experiment on the "Kal'mar" facility ($\lambda = 1$ μm, $l \approx 30$ μm, $r_{cr} \approx r_{bt}$, $\xi_0/F \ll 1$, $\alpha \approx 0.2$), we get $\xi_r^2/\xi_0^2 = 0.02$. A complete calculation shows that the fraction of resonance energy absorption is about 1% of the absorbed energy. This agrees with the fact that in these experiments a "contracting shell" is realized and the Rt diagram given in Fig. 6(b) is close to the experimental one.

We consider now the results of the calculations of variants connected with experiments on the "Janus" (Nd laser) setup.[11] The target is a glass shell, $R_0 = 43$ μm, $\Delta R_0 = 0.66$ μm. The laser energy $E_{pulse} = 30$ J in two beams, the shape of the pulse is an isosceles triangle with length along the base 146 ps. The target was positioned in the center between the focal planes of the two beams, and the distance ΔF between the foci was varied. We considered two focusing systems: $F/1$ ($2\xi_0 = F$) and "SIS," which consists of two aspherical mirrors (the angle of convergence of the rays was 163°).

We show in Fig. 8(a) the theoretical dependence of the fraction of absorbed energy E_{abs}/E_{pulse} on the quantity $\Delta F/2R_0$ (curves 1 and 2). The experimental values (points) are also shown there. For the two so greatly differing optical systems ($F/1$ and "SIS") we found agreement between theory and experiment. A characteristic feature is the presence of maxima in the absorbed energy, caused by the increase in the fraction of resonance absorption. A similar result is also obtained for the conditions of the experiment on the "Argus" setup.[11] The target is a glass shell, $R_0 = 52.5$ μm, $\Delta R_0 = 0.78$ μm, $E_{pulse} = 107$ J in two beams (Nd laser), the focusing system is $F/1$, and the radius of the beam at the target is 25 μm. The shape of the pulse is given in Fig. 8(b), curve 3. We also show there the time-dependence of the absorbed flux fraction $\Delta_{abs} = q_{abs}/q_{laser}$

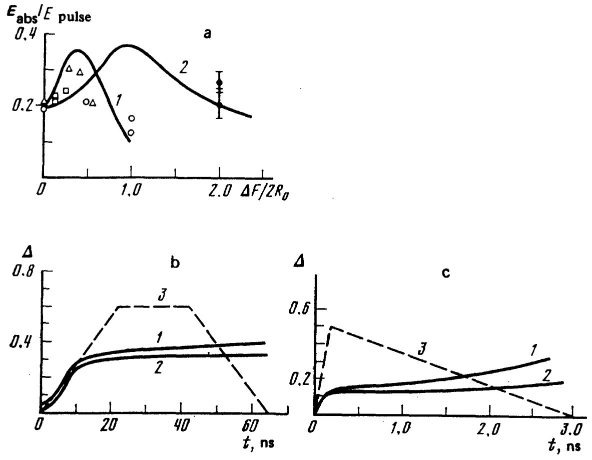

FIG. 8. Efficiency of absorption under experimental conditions: a) "Janus" set-up, curves: theory; points: experiment, curve 1 and open points for the optical system "SIS", curve 2 and filled points for the $F/1$ system; b and c) "Argus" and CO_2 laser, respectively: curves: 1) absorbed flux fractions, 2) resonance absorption flux fractions, 3) pulse shape.

(curve 1) and the fraction of the flux absorbed due to the resonance mechanism $\Delta^r_{abs} = q^r_{abs}/q_{laser}$ (curve 2). The fraction of energy absorbed was 34% of the laser energy. This agrees with the experimental value which is ~30%.[11] The fraction of absorbed resonance energy is ~90% of the absorbed energy.

Characteristic under the conditions considered is that thanks to the high flux densities (~10^{15} to 10^{16} W/cm^2) the shell is heated up by a thermal wave already before the moment of the collapse ("exploding shell" regime). Because of the short pulse length the plasma does not succeed in dispersing strongly and during the time it acts and the density gradient remains relatively large ($l \sim \lambda$). According to (28), the role of the resonance absorption mechanism then increases, $\xi_r/\xi_0 \sim 1$ during each laser pulse. Theory agrees with what is said about the heating of the target by epithermal electrons and about the heating of the shell by an electron heat-conduction wave.

We consider the results of the calculation of the heating and compression of the target under the conditions on a CO_2 laser.[12,13] In contrast to the "Argus" experiment, the compression regime is here determined solely by the heating of the target by the epithermal electrons. The parameters of the target and the pulse are: $R_0 = 105$ μm, $\Delta R_0 = 1.4$ μm (SiO_2, inside is DT gas with a density of 2×10^{-3} g/cm^3), $E_{pulse} = 380$ J, the shape of the pulse is shown in Fig. 8(c) (curve 3), the optical system is $F/2$, $r_{bt} = 75$ μm. We give in Fig. 8(c) the time-dependence of Δ_{abs} and Δ^r_{abs}. The laser light is in this case absorbed mainly via the resonance mechanism. The fraction of the absorbed energy is theoretically 0.19, experimentally 0.15 to 0.20.

A calculation assuming that the power resonantly absorbed is transferred by fast electrons and released in the target uniformly over the mass[14] gives for the time of collapse $t_c = 0.48$ ns, which agrees with experiment (0.5 ns). In that case $l \approx \lambda$, the plasma temperature (0.1 to 0.3 keV) is appreciably lower than in the ablation regime (~1 keV), and the corona disperses with a lower velocity. For instance, at times 0.25 ns and 0.48 ns r_{cr} is equal to 142 μm and 245 μm, respectively. For such plasma parameter values the role of the resonance absorption is, according to (28), large and there is practically no absorption due to the inverse bremsstrahlung mechanism. We note that an $l \sim \lambda$ inhomogeneity may arise also due to the light pressure on the reflection surface.[15,16]

In a calculation in which we neglected the heating by fast electrons we obtained a contracting shell regime, but the time of collapse in that case ($t_c = 1.45$ ns) did not agree at all with the experimental value.

The model considered of the absorption of laser light in spherical targets taking refraction into account, thus enables us to give an interpretation of existing experimental results, taking into account important effects which occur in actual experimental conditions.

The authors are grateful to A. S. Shikanov and A. A. Rupasov for useful discussions.

[1]Yu. V. Afanas'ev, N. N. Demchenko, O. N. Krokhin, and V. B. Rozanov, Zh. Eksp. Teor. Fiz. 72, 170 (1977) [Sov. Phys. JETP 45, 90 (1977)].
[2]M. Born and E. Wolf, Principles of Optics, Pergamon Press, Oxford, 1970.
[3]V. L. Ginzburg, Rasprostranenie elektromagnitnykh voln v plazme (Propagation of electromagnetic waves in a plasma) Nauka, 1967 [English translation published by Pergamon Press, Oxford].
[4]J. P. Friedberg, R. W. Mitchell, R. L. Morse, and L. I. Rudsinski, Phys. Rev. Lett. 28, 795 (1972).
[5]J. H. Erkkila, Laser Light Scattering and Absorption in Dense, Spherically Symmetric Plasmas, Ph.D. thesis, UCRL-51914, December, 1975.
[6]J. J. Thomson, C. E. Max, J. Erkkila, and J. E. Tull, Phys. Rev. Lett. 37, 1052 (1976).
[7]A. A. Samarskiĭ and Yu. P. Popov, Raxnostnye metody gazovoĭ dinamiki (Difference methods in gas dynamics), Nauka, 1975.
[8]N. G. Basov, A. A. Erokhin, Yu. A. Zakharenkov, N. N. Zorev, A. A. Kologrivov, O. N. Krokhin, A. A. Rupasov, G. V. Sklizkov, and A. S. Shikanov, Pis'ma Zh. Eksp. Teor. Fiz. 26, 581 (1977) [JETP Lett. 26, 433 (1977)].
[9]Yu. V. Afanas'ev, N. G. Basov, B. L. Vasin, *et al.*, Zh. Eksp. Teor. Fiz. 77, 2539 (1979) [Sov. Phys. JETP 50, 1229 (1979)].
[10]N. G. Denisov, Zh. Eksp. Teor. Fiz. 31, 609 (1956) [Sov. Phys. JETP 4, 544 (1957)].
[11]Laser Program Annual Report, Lawrence Livermore Lab., UCRL-50021, 1976, pp. 5–20.
[12]D. V. Giovanielli, G. H. McCall, and T. H. Tan, LA-UR-77-1703, Los Alamos Sc. Lab., 1977.
[13]C. W. Cranfill, LA-6827-MS, Los Alamos Sc. Lab., 1977.
[14]Yu. V. Afanas'ev, P. P. Volosevich, E. G. Gamaliĭ, N. N. Demchenko, O. N. Krokhin, and V. B. Rozanov, Preprint Lebedev Phys. Lab, Acad. Sc. USSR, No. 77, 1979.
[15]D. T. Attwood, D. W. Sweeney, J. M. Auerbach, and P. H. Y. Lee, Phys. Rev. Lett. 40, 184 (1978).
[16]P. Mulser and C. van Kessel, Phys. Rev. Lett. 38, 902 (1977).

Translated by D. ter Haar